

## WINDS IN OB-TYPE STARS

Lex Kaper

European Southern Observatory, Karl-Schwarzschild-Str. 2, D-85748 Garching bei München, Germany

### ABSTRACT

The International Ultraviolet Explorer satellite has made a tremendous contribution to the study of hot-star winds. Its long lifetime has resulted in the collection of ultraviolet spectra for a large sample of OB stars. Its unique monitoring capability has enabled detailed time-series analyses to investigate the stellar-wind variability for individual objects. IUE has also been a major driver for the development of the radiation-driven-wind theory; the synergy between theory and observations is one of the main reasons for the large progress that has been made in our understanding of hot-star winds and their impact on the atmospheres and evolution of massive stars.

Key words: hot stars; stellar winds; variability.

### 1. INTRODUCTION

OB-type stars, with masses ranging from about 8 to up to more than  $100 M_{\odot}$ , are hot ( $> 10,000$  K) and luminous ( $10^5 - 10^6 L_{\odot}$ ). The brightest supergiants with an absolute visual magnitude  $M_V = -9$  are visible up to the Virgo cluster ( $m_V = 22$ ) and thus potential candidates for the study of stellar populations in external galaxies. Because of their high luminosity, OB-type stars do not grow old (lifetime  $\sim 1 - 100 \times 10^6$  years) and thus trace star-forming regions.

From the shape of several strong spectral lines in their spectrum (like, e.g., the ultraviolet resonance lines of N v, Si iv, and C iv), it becomes immediately clear that OB stars lose a vast amount of material through a stellar wind. The blue edges of these so-called P Cygni-type profiles indicate maximum outflow velocities (few  $100 - 4000$  km/s) exceeding the surface escape velocity by a factor between 1 and 3 (Abbott 1978, Prinja et al. 1990). The associated mass-loss rates, most reliably measured from the stellar wind's free-free emission observed at radio wavelengths (Biegging et al. 1989), strongly depend on the OB-star's luminosity ( $\dot{M} \propto L^{1.6}$ ) and range from about  $10^{-9}$  to more than  $10^{-5} M_{\odot}/\text{yr}$ . Thus, during their lifetime OB stars lose a significant fraction of their initial mass, making mass loss a key ingredient in the description of their evolution (cf. Maeder

& Conti 1994, Chiosi 1998). Furthermore, hot-star winds play a dominant role in providing momentum, energy, and nuclearily processed material to the interstellar medium (Abbott 1982, Castor 1993).

In the following we will concentrate on the contribution of IUE to the study of hot-star winds. Why was the IUE satellite so important for this field of research? First of all, the main part of the OB-star spectrum is emitted in the far-UV, and, due to atomic physics, that is also the region where most of the important lines are situated. The UV resonance lines provide excellent diagnostics of the stellar-wind structure. Knowledge of the wind structure is essential if one wants to derive the stellar atmospheric parameters (cf. Kudritzki 1988), since practically all spectral lines are affected by the presence of a stellar wind. An important point we want to stress in this paper is that the success of IUE in this field of astronomy is for a substantial part based on the rapid and parallel progress made by theory. Each time a new IUE proposal had to be written we could report on the recent theoretical developments and predictions which could be tested with new observations.

The IUE archive contains high-resolution spectra ( $R = 10,000$ ) for a large sample of OB stars ( $\sim 400$ ), which has enabled the study of stellar-wind properties as a function of spectral type. Several atlases have been constructed showing the IUE spectra of O stars (Walborn et al. 1985), B stars (Rountree & Sonneborn 1993), and the UV P Cygni profiles of stars with spectral types between O3 and F8 (Snow et al. 1994). The "zoo" of OB stars contains many different species: "normal" OB main sequence stars, giants, supergiants; subdwarf OB stars (Heber); Wolf-Rayet stars (Willis); Luminous Blue Variables (Shore, Wolf); Central Stars of Planetary Nebulae; Be stars (Smith); B[e] stars;  $\beta$  Cep stars; magnetic B stars; hot binaries (Stickland); etcetera. Within brackets reference is made to the author of a contribution in these proceedings covering the respective type of stars; we will focus on the "normal" OB stars.

The second part of this paper deals with the variability aspect of hot-star winds, a topic that could be studied because of the unique monitoring capability of IUE. Mainly on the basis of IUE observations it could be demonstrated that variability is a fundamental property of radiation-driven winds, that it is not chaotic, but systematic, and that its characteristic timescale is determined by the stellar rotation period.

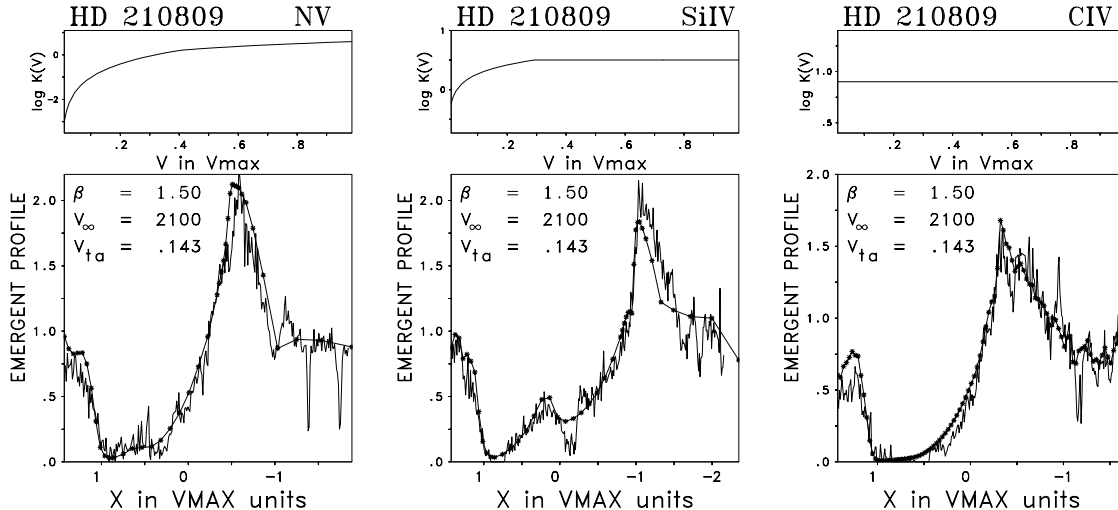


Figure 1. Radiative transfer fits of the ultraviolet (IUE) resonance lines of N V, Si IV, and C IV of the galactic O9 Iab supergiant HD210809. The x-axis is the velocity displacement measured from line center (blue doublet component) in units of  $v_\infty$ . The corresponding values for  $\beta$ ,  $v_\infty$ , and turbulent velocity  $v_{ta}$  are listed. The upper panels display the fit of the line strength stratification  $k(v) \propto \epsilon_{\text{abund}} X_{\text{ion}} \dot{M}$  as a function of velocity (from Haser 1995).

## 2. THE PHYSICS OF HOT-STAR WINDS

That the driving of hot-star winds is based on the interplay between gravity and the stellar radiation field becomes already apparent from the observed relation between the terminal velocity of the wind,  $v_\infty$ , and the escape velocity (Abbott 1978), and the relation between the mass-loss rate and stellar luminosity (Garmany & Conti 1984). In principle, one should be able to invert the latter relation in order to derive the luminosity, and thus the distance, from the observed mass-loss rate, were it not for the relatively large scatter in this relation.

Radiation-driven winds work on the principle that momentum contained in the stellar radiation field is transferred to gas particles in the wind via the scattering of photons. The main point is that momentum is a vector quantity and that the photons before scattering are all moving in one direction, i.e. away from the star, while they move in a “random” direction after the first scattering. The result is that the associated radiative force is directed away from the star. The scattering process takes place via spectral lines of the gas particles in the outer atmosphere. Lucy & Solomon (1970) were among the first to realize that the scattering of photons over a few strong (resonance) lines would result in a strong enough force to drive a wind. An essential ingredient is that the wind on its way out reaches velocities which are about a 100 times larger than the typical thermal width of the spectral lines, so that due to the doppler shift of the lines many more photons can be “tapped” compared to the static case. Castor, Abbott, and Klein (CAK, 1975) improved upon this result by incorporating also weak stellar lines, and were able to qualitatively reproduce the observed relations between  $v_\infty$  and  $v_{\text{esc}}$ , and between  $\dot{M}$  and L.

This was the state of the theory in the pre-IUE era. After the collection of ultraviolet spectra of many OB stars and measuring  $v_\infty$  and  $\dot{M}$  for a large sample

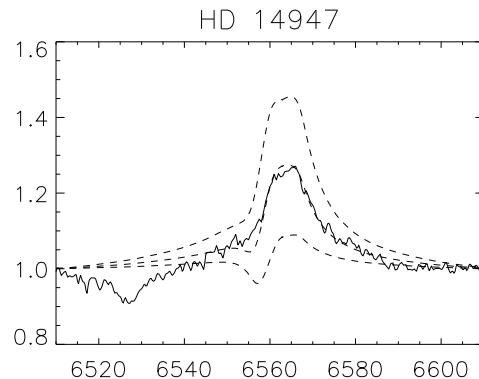


Figure 2.  $H\alpha$  profile (drawn line) of the O5 Iaf+ supergiant HD14947 compared with unified model calculations adopting  $10, 7.5,$  and  $5.0 \times 10^{-6} M_\odot/\text{yr}$ , respectively, for the mass-loss rate (Puls et al. 1996, figure from Kudritzki 1998).

of stars, it became clear that CAK theory had to be modified to quantitatively explain the observations. Independently, Friend & Abbott (1986) and Pauldrach, Puls, and Kudritzki (1986) improved on CAK theory by dropping some of the assumptions, the most important one being that the star is extended instead of a point source. Since then, radiation-driven wind theory has been further refined, in parallel with the development of non-LTE atmosphere models for hot stars; more than a million of different lines from over a hundred different ionic species are taken into account to calculate the radiative force (e.g. Pauldrach et al. 1994) and the resulting hydrodynamic structure of the stellar wind. It is now possible to model OB-star spectra quantitatively, consistently treating the photospheric and wind lines using so-called unified model atmospheres (cf. Kudritzki & Hummer 1990, Kudritzki 1998).

Figure 1 shows model fits to the UV resonance lines of the O9 Iab supergiant HD210809 (Haser 1995). An improvement with respect to the SEI method (Lamers et al. 1987, Groenewegen & Lamers 1989) is that Haser’s method allows a dependence of the turbulent velocity  $v_{ta}$  on velocity, which is predicted by theory (see below). The fits can be used to determine  $\dot{M}$ ,  $v_\infty$ , and the  $\beta$ -parameter (which defines the steepness of the velocity law). Although  $v_\infty$  can be derived very accurately (typically 5% accuracy), the determination of  $\dot{M}$  is very difficult, mainly because of the large uncertainty in the degree of ionization  $X_{\text{ion}}$ . Instead, the mass-loss rate can be much more precisely obtained from the H $\alpha$  profile (Puls et al. 1996). An example is given in Figure 2 for the O5 Iaf+ supergiant HD14947. A nice demonstration of the present state of the art is presented by Taresch et al. (1997), who model the most luminous and most massive star in our galaxy, HD93129A. One of their conclusions is that modelling of the far-UV spectrum is only possible when taking the interstellar absorption spectrum properly into account.

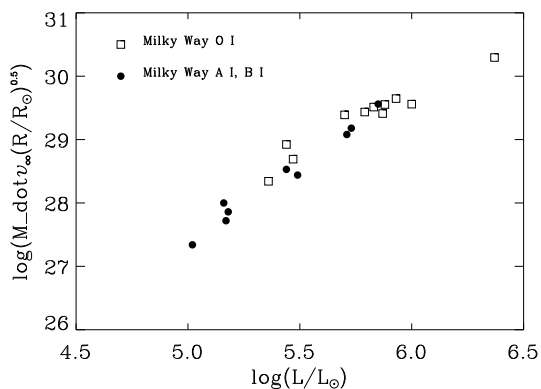


Figure 3. The observed Wind Momentum - Luminosity Relation for A-, B-, and O-supergiants in the Galaxy. All mass-loss rates have been determined from H $\alpha$ ; the terminal velocities were derived from the blue edges of UV P Cygni profiles (OB supergiants) or from H $\alpha$  (A supergiants). The figure is taken from Kudritzki (1998).

### 2.1. The Wind Momentum Luminosity Relation

As discussed in the previous section, the physics of hot-star winds strongly depend on the stellar radiation field. Would it be possible to determine the OB-star luminosity from its stellar-wind properties? In a recent review, Kudritzki (1998) argues that the observed relation between wind momentum ( $\dot{M}v_\infty$ ) and luminosity is very tight and can be used to derive distances to OB stars (see also Lamers & Leitherer 1993, Puls et al. 1996). Leaving out some terms with only a weak dependence on (other) stellar parameters, one obtains from theory a wind-momentum luminosity (WML) relation of the following form (Kudritzki 1998):

$$\dot{M}v_\infty \propto \frac{1}{\sqrt{R_\star}} L^{1/\alpha},$$

where  $\alpha \approx 2/3$  is a parameter which depends on the shape of the line strength distribution and the ion-

ization structure of the stellar wind. This already indicates that the WML relation should depend on metallicity.

Using the techniques described above, an empirical WML relation can be constructed by deriving  $\dot{M}$  and  $v_\infty$  from the spectra of a number of stars with known luminosity (and radius!). The result based on a sample of galactic supergiants of type A, B, and O is shown in Figure 3 (Puls et al. 1996, Kudritzki 1998). Indeed, a tight WML relation is observed, with possibly a slightly different slope for the O supergiants with respect to the A and B supergiants (filled circles). The empirical WML relation can be calibrated as a function of metallicity by observing blue supergiants in nearby galaxies with a different metallicity (e.g. LMC, SMC). When this has been done, the WML relation can be used to determine distances to blue supergiants beyond the local group, out to the Virgo and Fornax clusters of galaxies. Kudritzki (1998) argues that the uncertainties in distance modulus obtained with the WML method are comparable to those for individual Cepheids in galaxies if the period-luminosity relation is applied. The advantage of the WML method is that an individual reddening (and therefore extinction) can be derived for every object by comparing its observed colors with the model predictions. However, the possible impact of spectral variability (see section 3) on these results has to be investigated.

### 2.2. Instability of Radiation-Driven Winds

Radiation-driven winds are excellent laboratories for the study of radiation hydrodynamics; fundamental contributions to this field of physics stem from the observations of hot-star winds. Hydrodynamical, time-dependent (1-dimensional) simulations of radiation-driven winds have shown that the acceleration mechanism contains a potent instability. In their seminal paper, Lucy & Solomon (1970) already remarked that radiation-driven flows are unlikely to be steady. A small perturbation in velocity of a fluid element with respect to the surrounding gas will result in a strong increase (or decrease) of the acceleration of the ions in this element, because they are suddenly exposed to the unattenuated stellar continuum flux (or “shadowed” by the low-velocity wind closer to the star). This instability leads to the formation of shocks caused by high-velocity, low-density material running into low-velocity, high-density regions in front (Owocki et al. 1988, Owocki 1992). Thus, a radiation-driven wind is expected to be highly structured on relatively small scales.

The non-monotonic velocity and density structure of radiation-driven winds and the predicted formation of shocks provide a solution to a number of important observational facts: (i) the saturation of strong UV resonance lines; (ii) the observed soft X-ray emission of hot stars; and (iii) the observation of ions (e.g. O VI, N V) in the wind that cannot be explained by the temperature of the radiation field (so-called super ionization). Lucy (1982a) showed that in a shocked stellar wind a photon has to penetrate several (instead of one) “resonance zones” before it can escape. This explains the formation of P Cygni profiles with black absorption troughs (as in Figure 1, see Puls

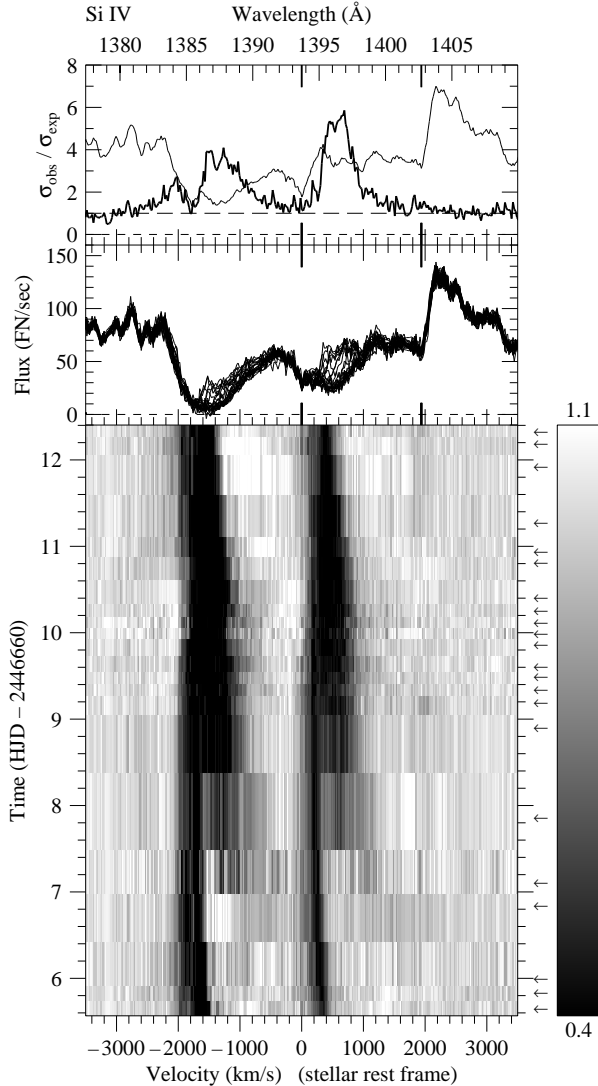


Figure 4. *19 Cep O9.5Ib* ( $v \sin i = 75$  km/s): Time series of the Si IV resonance doublet obtained in August 1986. The top panel displays the minimum-absorption template (thin line) used to produce the residual spectra shown in the grey-scale figure. The level of variability is indicated by a thick line. The middle panel shows an overplot of the spectral lines. In the lower panel the residual fluxes are converted into levels of grey; arrows denote mid-exposure times. A DAC appears at day 7 in both components of the doublet and slowly accelerates to its asymptotical velocity (from Kaper et al. 1996).

et al. 1993). The observed soft X-ray emission from hot stars (Chlebowski et al. 1989, Berghöfer et al. 1997) cannot be due to the star itself or a hypothetical corona since the stellar wind is optically thick at soft X-ray wavelengths. The X-ray emission has to originate in the outer wind regions. The existence (and interaction) of shocks in the wind could provide a natural explanation (Lucy 1982b, Feldmeier 1995). The super ionization might as well be the result of the produced X-ray flux in the wind (Pauldrach et al. 1994).

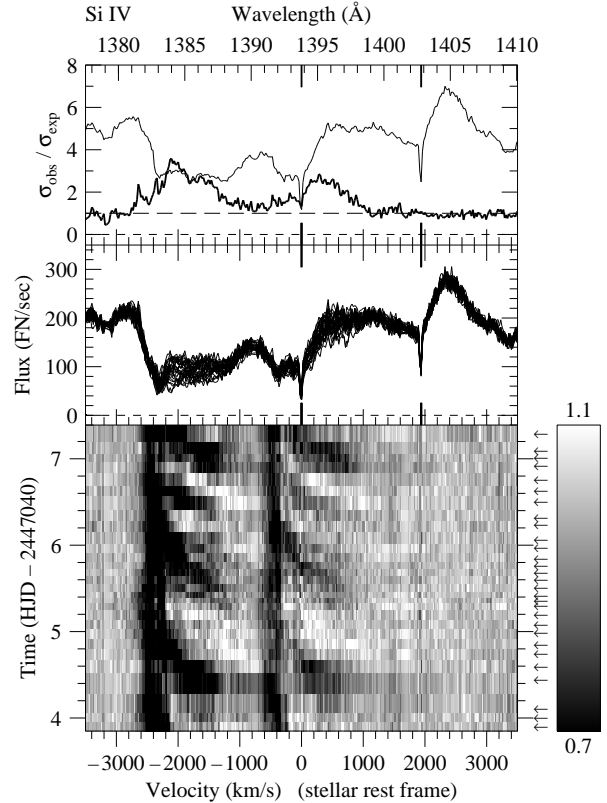


Figure 5. *68 Cyg O7.5 III:n(f)* ( $v \sin i = 274$  km/s): Time series Si IV resonance doublet (as Figure 4) obtained in September 1987. In both doublet components the appearance and evolution of 4 DAC events is witnessed. The absorption components reach an asymptotic velocity of 2400 km/s, i.e.  $v_{\infty}$ . The recurrence and acceleration timescale of the DACs is much shorter (1.4 day) compared to *19 Cep* in Figure 4 (from Kaper et al. 1996).

### 3. VARIABILITY IN HOT-STAR WINDS

IUE has proven to be a powerful tool for the study of variability in the supersonically expanding winds of hot stars. In particular, the blue-shifted absorption parts of the UV P Cygni lines show dramatic changes with time. Some of these profiles contain “narrow” absorption components, first recognized in *Copernicus* spectra of OB-type stars, at velocities close to the terminal velocity of the wind (e.g. Underhill 1975, Snow & Morton 1976). Lamers et al. (1982) reported the presence of narrow components in 17 out of 26 OB stars at a typical velocity of  $0.75 v_{\infty}$  and a mean width of about  $0.18 v_{\infty}$ . Later time-resolved studies with IUE (e.g. Henrichs 1984, Prinja & Howarth 1986, Henrichs 1988) showed that these narrow components are variable in velocity and profile. Continuous time series of UV spectra revealed that narrow components evolve from broad absorption features, which appear at low velocity and accelerate to higher wind velocities while narrowing (Prinja et al. 1987, Prinja & Howarth 1988, Henrichs et al. 1988). The current name of these variable absorption features is *discrete absorption components (DACs)*, which are the most prominent features of variability in hot-star winds. Because of their specific shape, DACs are readily recognized in single “snapshot” spectra. Howarth & Prinja (1989) detected DACs in more

than 80% of the IUE spectra in a sample of 203 galactic O stars. Grady et al. (1987) and Henrichs (1988) also found DACs in many Be stars, although not in non-supergiant B stars. Thus, the occurrence of DACs is a fundamental property of hot-star winds, and knowing how DACs develop is considered essential for our understanding of stellar-wind physics.

In search for the origin of stellar-wind variability, several monitoring campaigns have been organized with IUE. Since the typical timescale of variability is on the order of hours to days, continuous monitoring over a period of several days is essential. For this reason, dozens of NASA and ESA “shifts” had to be scheduled in sequence to the same observing program. On the basis of these observing campaigns it became clear that wind variability is systematic. Figures 4 and 5 show examples of the DAC behaviour in the Si IV resonance doublet of the O9.5 Ib supergiant 19 Cep and the O7.5 III giant 68 Cyg. The bottom panel gives a grey-scale representation of the evolution of DACs as a function of time (running upwards). The DACs start at low velocity ( $v_c = 0.2 - 0.5 v_\infty$ ) as broad absorption features and, while narrowing, move towards the blue until they reach an asymptotical velocity. This velocity is systematically lower (by 10-20%) than the maximum “blue edge” velocity observed in saturated P Cygni lines. The proposed solution is that the asymptotic DAC velocity has to be identified with the “real”  $v_\infty$  of the stellar wind and that the additional blue-shift in saturated P Cygni lines is caused by turbulence (i.e. the local spread in velocity due to the shocked wind structure, see section 2.2). Thus, DACs provide a diagnostic to measure  $v_\infty$ ; fortunately, Prinja et al. (1990) demonstrated that the so-called  $v_{\text{black}}$ , the last saturated point in a P Cygni profile measured in the direction of increasing blue-shift, shows a tight correlation with the corresponding asymptotic DAC velocity, so that it is still possible to obtain  $v_\infty$  from a single UV spectrum.

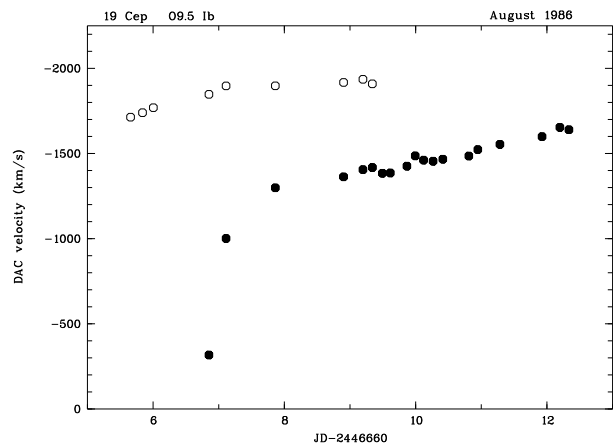


Figure 6. 19 Cep O9.5Ib: The DAC central velocity as a function of time in the Si IV resonance doublet (see Figure 4).

Obviously, in saturated resonance lines DACs cannot be observed; the steep blue edge of these profiles, however, often shows regular shifts of up to 10% in velocity, on a timescale comparable to that of the DACs. This edge variability is presumably related to the DAC behaviour; the observed differences in the asymptotic velocities of the DACs combined with

optical depth effects might cause the less regular behaviour of the high-velocity edges (cf. Kaper et al. 1998a).

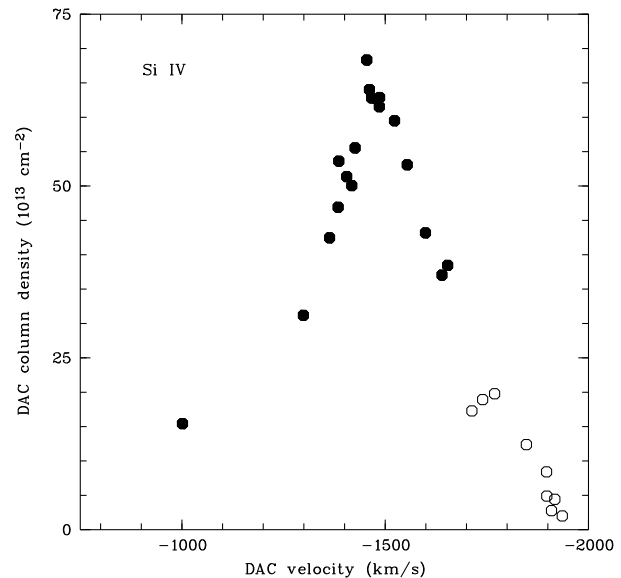


Figure 7. 19 Cep O9.5Ib: The corresponding change in DAC column density as a function of DAC central velocity in the Si IV resonance doublet. The column density peaks at  $0.75 v_\infty$ .

Figures 6 and 7 show the results of a quantitative analysis of the DAC behaviour in the Si IV resonance lines of 19 Cep (see also Figure 4). The migrating DACs were modelled in the way described by Henrichs et al. (1983) after division of the spectrum by a minimum-absorption template (Kaper et al. 1998a). The central velocity, central optical depth, width, and column density was measured for each pair of DACs in the UV resonance doublets. In Figure 6 a newly formed DAC accelerates towards the asymptotic velocity already reached by the narrow absorption component present from the beginning of the observing campaign. The acceleration is much slower than expected for a “normal”  $\beta = 1$  velocity law; the acceleration timescale appears to be longer for stars with a longer DAC recurrence timescale (see below). The corresponding change in column density is displayed in Figure 7. As is also found to be true in general, the DACs reach a maximum  $N_{\text{col}}$  at a velocity of about  $0.75 v_\infty$  and subsequently fade in strength. In cases where more than one resonance doublet was available to measure DACs, consistent results were obtained, supporting the interpretation that DACs correspond to changes in wind density and/or velocity rather than changes in the ionization structure of the stellar wind. It turns out that the DAC “pattern” is characteristic for a given star, but differences are found from year to year (e.g. the strength of the individual DACs, see Kaper et al. 1996, 1998a).

A key issue is the recurrence timescale of DACs; starting with Henrichs et al. (1988) and Prinja (1988), all papers in which more than one sequence of DACs is described, DACs repeat on a timescale comparable to the estimated rotation period of the star (cf. Kaper et al. 1996). As is illustrated by Figures 4 and 5, the star with the higher value of projected rotational velocity  $v \sin i$  (68 Cyg,  $v \sin i = 274$  km/s)

Table 1. Measured “wind” period in O star spectra compared to the estimated maximum rotation period (based on the stellar parameters listed by Howarth & Prinja (1989) and references therein). Runaway stars are indicated by (R). References: 1) Kaper 1993; 2) Prinja et al. 1992; 3) Howarth et al. 1993, 1995; 4) Fullerton et al. 1992: from He I 5876 Å; 5) Prinja 1988; 6) Stahl et al. 1996; 7) Kaper et al. 1997; 8) Kaper et al. 1998b.

Name	Sp. Type (Walborn)	$v \sin i$ (km s <sup>-1</sup> )	$R$ ( $R_{\odot}$ )	$P_{\max}$ (days)	$P_{\text{wind}}$ (days)		Reference
					UV	H $\alpha$	
$\zeta$ Oph (R)	O9.5 V	351	8	1.2	0.9		3
68 Cyg (R)	O7.5 III:n((f))	274	14	2.6	1.4	1.3	1,7
$\xi$ Per (R)	O7.5 III(n)((f))	200	11	2.8	2.0	2.0	1,7
$\lambda$ Cep (R)	O6 I(n)fp	214	19	4.5	1.3	1.2	1,7
$\zeta$ Pup (R)	O4 I(n)f	208	19	4.6	0.8	0.9	2,8
HD34656	O7 II(f)	106	10	4.8	1.1		1
15 Mon	O7 V((f))	63	10	8.0	> 4.5		1
63 Oph	O7.5 II((f))	80	16	10.2	> 3		5
HD135591	O7.5 III((f))	65	14	10.9		3.1	8
$\lambda$ Ori A	O8 III((f))	53	12	11.5	$\sim 4$	2.0:	1
$\theta^1$ Ori C	O6-O4 var	50:	12:	12:	“15.4”	15.4	6
19 Cep	O9.5 Ib	75	18	12.1	4.5	$\sim 5$	1,7
$\mu$ Nor	O9.7 Iab	85	21	12.5		6.0	8
$\alpha$ Cam (R)	O9.5 Ia	85	22	13.2		5.6	8
$\zeta$ Ori A	O9.7 Ib	110	31	14.3	$\sim 6$	6	1,8
10 Lac	O9 V	32	9	15.3	$\sim 7$		1
HD112244 (R)	O8.5 Ib(f)	70	26	18.8		6.2	8
HD57682 (R)	O9 IV	17	10	29.8		> 6	8
HD151804	O8 Iaf	50	35	35.4		2-3,7.3	4,8

shows DACs appearing with a much higher frequency than 19 Cep ( $v \sin i = 75$  km/s). Fourier analyses performed on the obtained datasets clearly reveal this periodicity (see, e.g., Kaper et al. 1998a). In Table 1 the observed “wind periods” (i.e., DAC recurrence timescales) are listed for a sample of O-type stars. The stars are ordered according to the estimated maximum rotation period:

$$P_{\max} = 50.6(v \sin i)^{-1} \left( \frac{R_{\star}}{R_{\odot}} \right) \text{ days},$$

where  $R_{\star}$  is the stellar radius. The table shows that stars with a shorter wind period end up higher on the list, consistent with the interpretation that the wind period relates to the rotation period of the star.

This strongly suggests that the regular appearance of DACs is related to the rotation of the star. The nature of this relationship has recently been the focus of a number of large IUE observing campaigns. During the IUE MEGA campaign (Massa et al. 1995) the WN5 star HD50896 (EZ CMa), the B0.5 Ib star HD64760, and the O4 If(n) star HD66811 ( $\zeta$  Pup) were monitored for a period of 16 days of nearly continuous observations in January 1995. The obtained time series for the Si IV resonance lines of HD64760 ( $v \sin i = 238$  km/s,  $P_{\max} = 4.8$  days) is shown in Figure 8. The three stars show continuous wind activity throughout the run with an apparent periodicity, which is coherent for at least a few rotation cycles (though not necessarily on longer intervals). Although the cyclical behaviour of wind variability is confirmed for the three target stars, the observations raise some important questions. In the case of  $\zeta$  Pup and HD64760, the regular pattern of DACs (recurrence timescale 0.8 and 1.2 days, respectively) seems to be superposed on a “slower” pattern of additional absorption. For  $\zeta$  Pup the slow pattern gives rise to a period of 5.2 days, which is interpreted as the rotation period of the star (Howarth et al. 1995).

In HD64760 such a “slow” period is not found. In fact, for HD64760 it turned out that the fast pattern is caused by almost sinusoidal modulations of the flux in stead of pure-absorption events. The features that we are used to call DACs make up the slow pattern, but a relation with the fast pattern in HD64760 is not evident (Prinja et al. 1995, Fullerton et al. 1997).

A new effect discovered in the spectra of HD64760 is the so-called phase bowing. Since the Fourier analysis is carried out for each wavelength point, the phase of the periodic variation is known as a function of velocity. A given phase of the modulation is first reached at an intermediate velocity of about 750 km/s and subsequently at both lower and higher velocities. Close inspection of Figure 8 reveals this effect as well. Inspired by Mullan (1986), Owocki et al. (1995) proposed that these characteristics naturally arise from absorption by strictly accelerating corotating wind streams seen in projection against the stellar disk. Cranmer & Owocki (1996) worked this out in more detail on the basis of hydrodynamical simulations. The Corotating Interaction Region (CIR) model, which was first applied to the solar wind, invokes fast and slow wind streams that originate at different locations on the stellar surface. Due to the rotation of the star, the wind streams are curved, so that fast wind material catches up with slow material in front, forming a shock at the interaction region. The shock “pattern” in the wind is determined by the boundary conditions at the base of the wind and corotates with the star. The wind material itself flows in a (nearly) radial direction under conservation of its angular momentum, but does *not* corotate with the star. It meets the interaction region at a distance from the star depending on a variety of parameters, including its original location on the stellar surface. Cranmer & Owocki induced an azimuthal variation in the outflow by a local increase or decrease in the radiative driving force, as would arise from a bright or dark “star spot” in the equatorial plane. Above

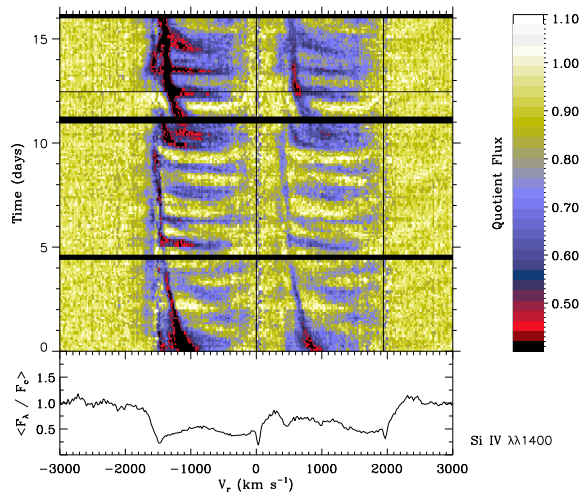


Figure 8. Time series of the Si IV resonance doublet of HD64760 ( $v \sin i = 238$  km/s) obtained in January 1995 during the IUE MEGA campaign. Time (in days from the beginning of the series) increases upward. The spectra were converted to a linear time grid by interpolation, and gaps appear whenever more than 5 hours elapsed between exposures. The individual spectra are normalized by a minimum absorption template so that all changes appear as absorption. The rest wavelengths of the doublet are shown as vertical lines. Note the apparent bowing of the black and white stretches (figure taken from Massa et al. 1995).

a bright spot the mass-loss rate is enhanced and the corresponding wind stream will reach a lower terminal velocity. The resulting wind structure is shown in Figure 9. Every time a CIR passes through the line of sight, a DAC is observed, explaining both the relation between the DAC recurrence timescale and stellar rotation and the observed phase bowing.

Also the  $H\alpha$  profiles of early-type stars indicate dramatic variability (Ebbets 1982). The origin of this variability has to be understood given the importance of this line for mass-loss determinations (section 2.1). Kaper et al. (1997) show that for their sample of O-type stars, simultaneous ultraviolet and  $H\alpha$  observations reveal the same periodicity and are consistent with the CIR model. Thus, wind variability also affects the  $H\alpha$  line, although for main sequence stars the line is too weak to detect variability. In Table 1 a comparison is made between the wind periods derived from the UV P Cygni lines and the  $H\alpha$  profile. The results of a search for wind variability in the  $H\alpha$  line for a large sample ( $\sim 70$ ) of O-type stars will be presented in Kaper et al. (1998b).

In conclusion, the CIR model seems to be the best explanation for the observed wind variability. The origin of the bright or dark spots on the stellar surface is, however, not known. The two obvious candidates are non-radial pulsations and surface magnetic fields. Reference is made to the contribution by Henrichs in this volume for a more detailed interpretation of the cyclical variability in hot-star winds.

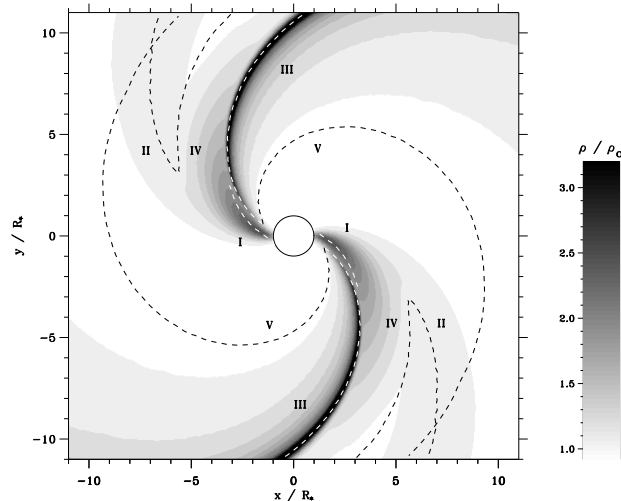


Figure 9. Example of the large-scale wind structure produced by the CIR model of Cranmer & Owocki. The density structure of the stellar wind in the equatorial plane (normalized to the “unperturbed” wind density) is shown for the case of the Bright Spot model. Area I indicates the enhanced mass flux above the bright spot, area III is the CIR compression. According to their model, the largest relative contribution to the Sobolev optical depth (producing DACs in line profiles) comes from region V, the so-called radiative acoustic Abbott kink (figure from Cranmer & Owocki (1996).

## ACKNOWLEDGEMENTS

I would like to thank my colleagues Huib Henrichs, Joy Nichols, Jeroen de Jong, Alex Fullerton, Joachim Puls, Stan Owocki, and John Telting for the nice collaboration. The IUE Observatory staff at both Goddard and Vilspa are acknowledged for their dedicated efforts in executing these difficult programs. I thank the Organizing Committee for the invitation to present this paper.

## REFERENCES

- Abbott, D.C. 1978, ApJ 225, 893
- Abbott, D.C. 1982, ApJ 263, 723
- Berghöfer, T.W., Schmitt, J.H.M.M., Danner, R., Cassinelli, J.P. 1997, A&A 322, 167
- Biegging, J.H., Abbott, D.C., Churchwell, E.B. 1989, ApJ 340, 518
- Castor, J.I. 1993, in ASP Conf. Ser. 35, Eds. Cassinelli, Churchwell, p. 297
- Castor, J.I., Abbott, D.C., Klein, R.I. 1975, ApJ 195, 157
- Chiosi, C. 1998, in Proc. 8<sup>th</sup> Canary Winter School 1996, Eds. Aparicio, Herrero, Cambridge Univ. Press
- Chlebowski, T., Harnden, F.R.Jr., Sciortino, S. 1989, ApJ 341, 427
- Cranmer, S.R., Owocki, S.P. 1996, ApJ 462, 469
- Ebbets, D. 1982, ApJS 48, 399
- Feldmeier, A. 1995, A&A 299, 523
- Friend, D.B., Abbott, D.C. 1986, ApJ 311, 701

- Fullerton, A.W., Gies, D.R., Bolton, C.T. 1992, ApJ 390, 650
- Fullerton, A.W., et al. 1997, A&A 327, 699
- Garmany, C.D., Conti, P.S. 1984, ApJ 284, 705
- Grady, C.A., Bjorkman, K.S., Snow, T.P. 1987, ApJ 320, 376
- Groenewegen, M.A.T., Lamers, H.J.G.L.M. 1989, A&A 79 359
- Haser, S.M. 1995, PhD thesis Univ. of Munich
- Henrichs, H.F. 1984, in Proc. 4th Europ. IUE Conf., ESA SP-218, p. 43
- Henrichs, H.F. 1988, NASA/CNRS "O, Of and Wolf-Rayet Stars", Eds. Conti & Underhill, p. 199
- Henrichs, H.F., Hammerschlag-Hensberge, G., Howarth, I.D., Barr, P. 1983, ApJ 268, 807
- Henrichs, H.F., Kaper, L., Zwarthoed, G.A.A. 1988, in "A Decade of UV Astronomy with the IUE Satellite" (ESA SP-281), Vol.2, p.145
- Howarth, I.D., Prinja R. 1989, ApJS 69, 527
- Howarth, I.D., et al. 1993, ApJ 417, 338
- Howarth, I.D., Prinja, R.K., Massa, D. 1995, ApJ 452, L65
- Kaper, L. 1993, PhD thesis Univ. of Amsterdam
- Kaper, L., et al. 1996, A&AS 116, 257
- Kaper, L., et al. 1997, A&A 327, 281
- Kaper, L., Henrichs, H.F., Nichols, J.S., Telting, J.H. 1998a, A&A, submitted
- Kaper, L., et al. 1998b, to be submitted to A&A
- Kudritzki, R.P. 1988, in "Radiation in moving gaseous atmospheres", Saas-Fee 1988
- Kudritzki, R.P. 1998, in Proc. 8<sup>th</sup> Canary Winter School 1996, Eds. Aparicio, Herrero, Cambridge Univ. Press
- Kudritzki, R.P., Hummer, D.G. 1990, ARA&A 28, 303
- Lamers, H.J.G.J.M., Gathier, R., Snow, T.P. 1982, ApJ 258, 186
- Lamers, H.J.G.L.M., Cerruti-Sola, M., Perinotto, M. 1987, ApJ 314, 726
- Lamers, H.J.G.L.M., Leitherer, C. 1993, ApJ 412, 771
- Lucy, L.B. 1982, ApJ 255, 278
- Lucy, L.B. 1982, ApJ 255, 286
- Lucy, L.B., Solomon, P. 1970, ApJ 159, 879
- Maeder, A., Conti, P.S. 1994, ARA&A 32, 227
- Massa, D., et al. 1995, ApJ, 452, L53
- Mullan, D.J. 1986, A&A 165, 157
- Owocki, S.P. 1992, in "The Atmospheres of Early-Type Stars", Eds. Heber & Jeffery, Springer Berlin, p. 393
- Owocki, S.P., Castor, J.I., Rybicki, G.B. 1988, ApJ 335, 914
- Owocki, S.P. Cranmer, S., Fullerton, A.W. 1995, ApJ 453, L37
- Pauldrach, A.W.A., Puls, J., Kudritzki, R.P. 1986, A&A 164, 86
- Pauldrach, A.W.A., et al. 1994, A&A 283, 525
- Prinja, R.K. 1988, MNRAS 231, 21P
- Prinja, R.K., Howarth, I.D. 1986, ApJS 61, 357
- Prinja, R.K., Howarth, I.D., Henrichs, H.F. 1987, ApJ 317, 389
- Prinja, R.K., Howarth, I.D. 1988, MNRAS 233, 123
- Prinja, R.K., Barlow, M.J., Howarth, I.D. 1990, ApJ 361, 607
- Prinja, R.K., et al. 1992, ApJ 390, 266
- Prinja, R.K., Massa, D., Fullerton, A.W. 1995, ApJ 452, L61
- Puls, J., Owocki, S.P., Fullerton, A.W., 1993, A&A, 279, 457
- Puls, J., et al. 1996, A&A 305, 171
- Rountree, J., Sonneborn, G. 1993, NASA Ref. Pub. 1312
- Snow, T.P., Morton, D.C., 1976, ApJS 32, 429
- Snow, T.P., Lamers, H.J.G.L.M., Lindholm, D.M., Odell, A.P. 1994, ApJS 95, 163
- Stahl, O., et al. 1996, A&A 312, 539
- Taresch, G., et al. 1997, A&A 321, 531
- Underhill, A.B. 1975, ApJ 199, 691
- Walborn, N.R., Nichols-Bohlin, J., Panek, R.J. 1985, NASA Ref. Pub. 1155